RESEARCH ARTICLE

JOURNAL OF Applied Polymer SCIENCE **WILEY**

Development of nystatin-based antifungal, biodegradable polymer composite materials for food packaging via. melt processing approach

Rituparna Duarah[1] | Ivana Aleksic[2] | Dusan Milivojevic[2] |
Saranya Rameshkumar[3] | Jasmina Nikodinovic-Runic[2] |
Ramesh Babu Padamati[1,3]

[1]School of Chemistry, BiOrbic Bioeconomy SFI Research Centre, Trinity College Dublin, Dublin, Ireland

[2]Institute of Molecular Genetics and Genetic Engineering, University of Belgrade, Belgrade, Serbia

[3]School of Chemistry, CRANN and AMBER SFI Research Centre, Trinity College Dublin, Dublin, Ireland

Correspondence
Jasmina Nikodinovic-Runic, Institute of Molecular Genetics and Genetic Engineering, University of Belgrade, Vojvode Stepe 444a, 11221 Belgrade, Serbia.
Email: jasmina.nikodinovic@imgge.bg.ac.rs

Ramesh Babu Padamati, BiOrbic Bioeconomy SFI Research Centre, School of Chemistry, Trinity College Dublin, D2 Dublin, Ireland.
Email: babup@tcd.ie

Abstract

Novel bio-based, biodegradable packaging material was developed with multi-functional properties of good mechanical strength, potent biocompatibility, and antifungal attributes, predominantly against fungi vital in food spoilage. Biodegradable polymer composites were prepared with a natural antifungal agent, nystatin (Nyst), by melt processing technique for the first time. Initially, Polycaprolactone (PCL) was melt-mixed with various percentages of nystatin to produce nystatin-encapsulated PCL composites (PCL/Nyst). The as-prepared PCL/Nyst composites were melt-mixed with polylactic acid (PLA) to produce nystatin PLA/PCL blend composites. Subsequently, the prepared composites were compression molded in the form of films (1 mm) for further characterization. The composite's structural properties were evaluated by SEM, FTIR, mechanical and thermal studies. In addition, the composites were tested in vitro against a panel of pathogenic fungi and for antibiofilm attributes, specifically against three *Candida* species (*C. albicans* ATCC10231, *C. parapsilosis* ATCC22019, and *C. glabrata* ATCC2001), and foodborne *Penicillium* sp. All the composites containing 2 to 20 wt% nystatin displayed good activity and sustained nystatin release for up to 4 days. Thus, the overall study demonstrates the potential application of natural antifungal agents in biodegradable polymers to produce novel composite films for antimicrobial packaging without inducing any toxicity, judged from the toxicity assay using nematode *Caenorhabditis elegans*.

KEYWORDS
antifungal, melt-mixing technique-biodegradable blends-packaging-antifungal properties, nystatin, polycaprolactone, polylactic acid

1 | INTRODUCTION

Globally, food safety, and quality are of major concern for producers and consumers. Food spoilage due to fungal contamination is one of the key issues that cause the inevitable loss of food products even before their consumption.[1,2] Fungal contamination accelerates food spoilage and also generates mycotoxins causing allergies and infections in humans. Processing techniques, such as irradiation, thermal processing, high-pressure treatment, and freezing are commonly used to maintain the quality and shelf life of the products; however, foods contaminated by pathogens pose a serious risk to human health. Nearly one-quarter of food waste is linked to microbial contamination resulting in loss of nutrition, taste, and quality.[3] Food spoilage not only threatens food security but also leads to greenhouse gas emissions. Roughly one-third of food produced is wasted, and waste food generates 10% of global greenhouse gas emissions.[4] Hence, the growing demand for maintaining food safety and quality in recent years necessitates developing novel food packaging materials. With increasing consumer awareness on sustainable packaging materials, there has been a huge momentum toward producing biodegradable polymer-based packaging materials.[5,6]

Recent progress and advances in biodegradable polymers have created an effective shift in achieving desirable mechanical properties and their potential application in active food packaging technology.[7,8] Active or intelligent food packaging materials composed of robust blends of biodegradable polymers and safe antimicrobial agents are expected to extend the shelf-life of food products.[9] Innovative packaging materials composed of blends of bio-based materials are expected to replace fossil-based packaging products with improved sustainability. However, the properties of biodegradable polymers, such as elongation, barrier properties, and thermal stability, make it challenging to use these polymers in various applications.[10–14] Various strategies have evaluated, such as the use of plasticisers,[15,16] additives,[17] crosslinking,[18] and polymer blending[15,19–22] to improve the properties of biodegradable polymers. Using biodegradable polymers for packaging applications results in a smaller carbon footprint and increases consumers' acceptance while maintaining the food safety and nutritional quality of packaged food products.[23] Thus, the synergistic efficiency of active and biodegradable food packaging materials is expected to maintain both food safety and sustainability. Therefore, research has focused on incorporating naturally derived antifungal agents into bio-based composites. Naturally derived polyenes are the oldest class of antifungal drugs among which antifungal agent, Nystatin has attracted significant interest due to its inhibitory action against various wide pathogenic and non-pathogenic fungi and yeast.[24,25] Nystatin is known for its superior antifungal properties and is a potential additive to improve active food packaging materials' quality and shelf life.

Biodegradable polymers modified with polyene compounds are emerging as promising food packaging materials with remarkable anti-fungal properties.[26,27] Integrating suitable antifungal agents into a biodegradable polymer matrix enhances the shelf-life and product quality by inhibiting the growth of fungal species on the food surface. It is also critical to maintain the specific proportion of chosen antifungal agent considering its inhibitory activity and how it is supplemented into the polymer material.[28] The design of antifungal-based biodegradable packaging materials is mainly done with the aim of releasing the antifungal agents which had been incorporated in advance. Implementation of such active packaging materials is conducted primarily via. two processes: (a) solvent casting techniques, (b) solvent-free processing techniques, such as extrusion or melt-blending. In solvent casting, a polymeric matrix is solubilized in an appropriate solvent with the active components to form a film-forming solution to be sprayed or cast onto a suitable substrate. Pekmezovic et al. synthesized mcl-PHA/antifungal polyene films with nystatin and amphotericin B via solvent casting, which exhibited good hydrophobicity.[26] However, the thermal properties of the films were unaffected by the incorporation of polyenes. All PHA films prevented biofilm formation against *C. albicans*, although they proved inefficient in eliminating mature biofilms. Bargan et al. synthesized hydroxyapatite and nystatin-based cellulose acetate composites via phase inversion, which exhibited improved local therapeutic effects in candidiasis therapy.[29] The nystatin-based composites exhibited a strong inhibition effect on the *Candida albicans* growth, suggesting their clinical potential application with a great appeal toward the treatment of localized infections. On the other hand, melt-blending technique involves processing in a molten state, thus ensuring homogeneous mixing of polymer and active additives. Wangprasertkul et al. produced antimicrobial biodegradable packaging using sodium benzoate and potassium sorbate based on poly(butylene adipate-co-terephthalate) and thermoplastic starch blends (PBAT/TPS) via blown-film extrusion. The films displayed active antimicrobial functions that effectively inhibited microbial growth in fresh rice noodles, however, these additives are fossil-based resources.[30] On the other hand, polyene compounds, such as nystatin are natural antifungal agents, which are thermally non-stable and get partially volatilized during the melt processing with polymer composites resulting in either loss of or proportionally undesirable release of anti-fungal activity.[31]

In this regard, several strategies have been investigated to preserve antifungal activity by introducing polymer matrices specifically in the form of plasticizers, microporous carriers, or encapsulation.[32] Previous literature

suggests an alternative in the form of coating an extra layer in a molten state at a lower temperature using polymeric sealants or copolymers.[33–35] However, as per our knowledge, there are no reports on polyene-based biodegradable composites prepared by melt-processing technique. So, the present work aims to develop melt mixing process with naturally derived nystatin and biodegradable polymer blends constituting polycaprolactone (PCL) and polylactic acid (PLA). Raising attention toward using completely biodegradable plastic food packaging has immensely drawn research interest in applying PCL/PLA blends for antimicrobial packaging.[36,37] To overcome the trade-off between the mechanical properties of PCL and PLA and the low thermal stability of nystatin, this research presents a novel approach of melt-mixing PCL with different weight percentages of nystatin to form nystatin-based PCL composites (PCL/Nyst) composite and PLA via. melt processing technique to elevate the diverse material performance and impart antifungal properties. This technique has proven to be very effective in enhancing the toughness of a brittle polymer like PLA by blending it with ductile, soft polymers (in this case PCL/Nyst composites) to develop tough blend composites of PLA/PCL/Nystatin (PLA/PCL/Nyst) with a minimum reduction of its stiffness. Furthermore, PLA/PCL/Nyst composites can combine the synergistic attributes of good flexibility and antifungal property. In this current investigation, the performance of PLA/PCL/Nyst blend composites is also compared with virgin PCL and PLA blends to validate the superiority of the former as a high-performing, sustainable and tough antifungal food packaging material.

2 | EXPERIMENTAL

2.1 | Materials

Polycaprolactone (PCL, CAPA6500, molecular weight $\sim$ 50,000, supplied by Perstorp), Polylactic acid (PLA, Biopolymer-4043D, molecular weight: 110.000 g/mol, supplied by Nature Works, USA), nystatin (powder, 90% of the particles <10 μm; and 100% of the particles <15 μm, Sigma Aldrich). Nystatin was stored at −1°C. Both PLA and PCL pellets were vacuum dried at 80 and 40°C, respectively, for 5 and 2 h respectively; Phosphate buffer solution (PBS of pH 5.5 and 7, Sigma Aldrich).

2.2 | Preparation of PCL/Nyst composites

PCL/Nyst composites were successfully produced by melt-processing technique for the first time. In a typical process, PCL was melt-mixed with different weight percentages (2%, 5%, 10%, and 20%) of nystatin using a lab-scale Brabender melt-mixer at 100°C and 50 rpm for 10 min as given in Table 1. The processed samples were encoded as PCL/Nyst2%, PCL/Nyst5%, PCL/Nyst10%, and PCL/Nyst20%. The PCL/Nyst composites will be utilized to fabricate PLA composites.

2.3 | Preparation of PLA/PCL/Nyst composites

In a similar method, PLA/PCL/Nyst composites were prepared by melt-mixing PLA and PCL-Nyst using a Brabender melt-mixer at 180°C and 50 rpm for 10 min as given in Table 2. First, PLA pellets were allowed to mix for 4 min, thereafter, PCL-Nyst composite was added (based on the wt% of nystatin required) to the mixture and further processed for 6 min. The processed samples were encoded as PLA/PCL/Nyst2.5%, PLA/PCL/Nyst6.5%, and PLA/PCL/Nyst10%, containing 2.5, 6.5, and 10 wt% nystatin, respectively. Pristine PLA, PCL, and PLA/PCL composites were also prepared for comparison purposes.

2.4 | Characterization of materials

The melt-processed samples were compression molded to $10 \times 10 \times 0.1$ cm rectangular specimens at 180°C under optimized pressure conditions using a compression press (Servitech Polystat 200 T, Wustermark, Germany). The plastic sheets were punched with a cutter to dumbbell-shaped samples with dimensions of 75 mm $\times$ 4 mm $\times$ 1 mm and were used for stress–strain measurements.[38] Tensile measurements were carried out using a Zwick twin-column tensile tester with a 2.5 kN load cell. The tensile tests were carried out at room temperature and a cross-head speed of 25 mm/min. Young's modulus, ultimate tensile strength, breaking strength, elongation at break and toughness values were calculated by integrating the stress–strain data obtained from the best triplicate measurement. The glass transition temperature (T_g) and melting temperature (T_m) of polymers and biodegradable plastics were analyzed using a PerkinElmer Pyris Diamond calorimeter calibrated to indium standards. The samples were sealed in aluminum pans and heated from −70 to +200°C at a rate of 10°C/min. The samples were run through a first heating and cooling cycle to remove the thermal history. The percentage of crystallinity is determined using the following equation.[39]

$$X_c \ (\%\mathrm{Crystallinity}) = \frac{\Delta Hm}{w \times \Delta Hm^{\circ}} \times 100\%$$

TABLE 1 Composition of PCL composites with different weight % of nystatin.

Composites		Mass fraction (wt%)	Weight (g)
PCL/Nys2%	nystatin	2	0.8
	PCL	98	39.2
PCL/Nys5%	nystatin	5	2
	PCL	95	38
PCL/Nys10%	nystatin	20	4
	PCL	80	36
PCL/Nys20%	nystatin	10	8
	PCL	90	32

TABLE 2 Composition of PLA composites with different weight % of PCL/Nyst.

Composites		Mass fraction (wt%)	Weight (g)
PLA/PCL	PLA	80	32
	PCL	20	8
PLA/PCL/Nyst2.5%	PLA	75	30
	PCL/Nyst10%	25	10
PLA/PCL/Nyst6.5%	PLA	68.75	27.5
	PCL/Nyst20%	31.25	12.5
PLA/PCL/Nyst10%	PLA	50	20
	PCL/Nyst20%	50	20

ΔHm = specific melting enthalpy, ΔHm^o is the melting enthalpy of 100% crystalline virgin polymer (where the melting enthalpy of 100% PLA is 93.7 J/g), and w = weight fraction of PCL or PLA phase in PCL/PLA blends.

A PerkinElmer 4000 thermal instrument was used to carry out the thermogravimetric study in the range of temperature (25–800)°C, at a scanning rate of 10°C/min, keeping up an inert atmosphere of nitrogen (at 30 mL/min flow rate). The FTIR spectra of the prepared nanocomposites and nanomaterials were recorded on a Nicolet FTIR spectrophotometer (Impact-410, Madison, USA).

2.5 | Statistical analysis

The results are presented as average ± standard deviation (*SD*). Statistical analysis was done by comparing the average values using a one-way Analysis Of VAriance (ANOVA, Single Factor), with Fisher's Least Significant Difference (LSD) post-hoc test. The level of statistical significance is expressed as a *p*-value (probability value), and $p \leq 0.05$ was considered statistically significant. Statistical analysis tests were performed in Microsoft Excel Spreadsheet Software by Data Analysis Tools add-in.

2.6 | Scanning electron microscopy (SEM)

The cross-section SEM morphology of the composites was imaged with the help of a field emission scanning electron microscope (Zeiss Ultra SEM). Samples for cross-sectional imaging were prepared by fracturing the films under liquid nitrogen. The films were coated with gold–palladium (Au-Pd) sputtering to impart conductivity and visualize the blended segments better. For SEM analysis, an accelerating voltage between 3 and 5 kV was fixed with a secondary electron (SE2) detector to capture images at various magnifications ($100\times$, $500\times$, $1000\times$).

2.7 | Determination of the antifungal activity of PLA, PCL, and PLA/PCL blend composites

2.7.1 | Agar disk-diffusion method

Direct assay for evaluating antifungal activity by detecting growth inhibition zone is based on the standard disk diffusion method used in medicinal and scientific laboratories.[40] Overnight cultures of *Candida* species all obtained from American Type Culture Collection (ATCC), *Candida*

albicans ATCC10231, *Candida parapsilosis* ATCC22019 and *Candida glabrata* ATCC2001 were made in Sabouraud dextrose agar (SDA) liquid medium,[41] incubated on 37°C on a rotary shaker at 180 rpm. After, SAB agar plates were inoculated with a standardized inoculum of overnight cultures of *Candida* species. Plastic materials were cut into approximately the same pieces (1 × 1 cm), sterilized in 70% ethanol, air dried and placed on the top of the SAB agar plates. Plates were incubated in an upright position at 37°C for 24 h. Additionally, plastic materials were tested on foodborne *Penicillium* sp. from in-house collection (isolated from spoiled lemon) whereby spore suspension was used to inoculate SAB plates.

2.7.2 | Broth-microdilution assay of material extracts

A standardized methodology for the determination of minimum inhibitory concentration (MIC) values used in this study is recommended by the National Committee for Clinical Laboratory Standards (M07-A8) for bacteria and Standards of European Committee on Antimicrobial Susceptibility Testing (v 7.3.1: Method for the determination of broth dilution minimum inhibitory concentrations of antifungal agents for yeasts) for *Candida* spp.[42] The plastic materials where incubated in SAB medium (100 mg/mL) on 37°C on rotary shaker at 180 rpm. Those extracts were used for the assessment of antibacterial activity in this assay. The concentration gradient was expressed in percentages, with the highest tested percentage of 50% (v/v) with the serial dilutions up to 0.39% (v/v). The inoculums were 1×10^5 colony-forming units, cfu/mL for fungal species. The MIC value was recorded as the lowest concentration that inhibited the growth after 24 h at 37°C, using the Tecan Infinite 200 Pro multi-plate reader (Tecan Group Ltd., Männedorf, Switzerland).

2.8 | Release kinetics of Nyst

The composite films (PCL/Nyst2%, PCL/Nyst5%, PCL/Nyst10%, PCL/Nyst20%, PLA/PCL/Nyst2.5%, PLA/PCL/Nyst6.5%, and PLA/PCL/Nyst10%) were cut into small rectangular shapes in (3 × 1) cm² dimensions and placed in 10 mL of Phosphate Buffered Saline (pH: 7) solution in separate glass bottles at 39° under mechanical agitation. Aliquots (3 mL) were drawn at specific time intervals and replaced with fresh 3 mL PBS solution concurrently. The withdrawn samples were directly filtered through Whatman filter paper and assayed spectrophotometrically for nystatin content in triplicate by a UV/VIS spectrophotometer at a maximum absorption wavelength, λ_{max}, 290 nm,

using a standard calibration curve. The study to determine the release of nystatin from the 7 composite films was conducted over a period of 4 days. The cumulative amount of nystatin released into the solution was measured at preset time intervals and reported based on two individual experiments.[26]

2.9 | Caenorhabditis elegans survival assay

C. elegans N2 (glp-4; sek-1) was propagated under standard conditions, synchronized by hypochlorite bleaching, and cultured on nematode growth medium using *E. coli* OP50 as a food source, as described previously.[42–44] The *C. elegans* survival assay was carried out as described previously with minor modifications. In brief, synchronized worms (L4 stage) were suspended in a medium containing 95% M9 buffer (3 g of KH_2PO_4, 6 g of Na_2HPO_4, 5 g of NaCl, and 1 mL of 1 M $MgSO_4$ in 1 liter of water), 5% LB broth (Oxoid), and 10 μg of cholesterol (Sigma-Aldrich) per mL. Material extracts were prepared as described previously in section 2.4.2. Fifity μL of this suspension of nematodes (25–35 nematodes) were transferred to the wells of a 96-well microtiter plate where 50 μL of sterile medium were added to the control while 50 μL media containing increasing concentrations of material extracts: 12.5%, 25%, 50%, and 100% (v/v) were added to the tested wells. The plates were incubated at 25°C for 48 h. The fraction of dead worms was determined by counting the number of dead worms and the total number of worms in each well using a stereomicroscope (SMZ143-N2GG, Motic, Germany). The material extracts were tested at least three times in each assay, and each assay was repeated at least two times ($n \geq 6$).

3 | RESULTS AND DISCUSSION

3.1 | Preparation of PCL/Nyst and PLA/PCL/Nyst composites

The PCL/Nyst composites were prepared by melt-mixing technique using PCL and nystatin, as shown in Table 1. The extent of interaction between nystatin and PCL depends on the level of nystatin dispersion into the PCL matrix. Intially four different types of composites were prepared namely, PCL/Nyst composites, by melt-blending PCL with 2%, 5%, 10%, and 20% weight percentages of nystatin, encoded as PCL/Nyst2%, PCL/Nyst5%, PCL/Nyst10%, and PCL/Nyst20%, respectively. Similarly, PLA/PCL/Nyst composites were formed by melt-mixing PCL/Nyst with PLA. In this context, the dispersion of

TABLE 3 Composition of PLA/PCL/Nyst composites.

Composites		Mass fraction (wt%)	Weight (g)
PLA/PCL/Nyst2.5%	PLA	75	30
	PCL/Nyst10%	25	10 (PCL = 9 g; nystatin = 1 g)
PLA/PCL/Nyst6.5%	PLA	68.75	27.5
	PCL/Nyst20%	31.25	12.5 (PCL = 10 g; nystatin = 2.5 g)
PLA/PCL/Nyst10%	PLA	50	20
	PCL/Nyst20%	50	20 (PCL = 16 g; nystatin = 4 g)
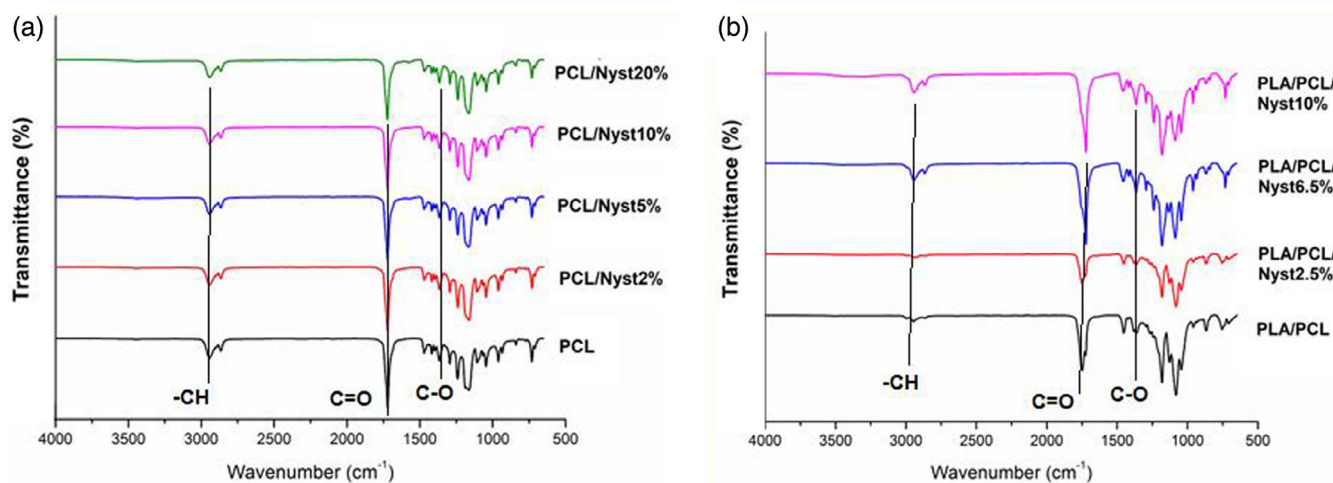
FIGURE 1 FTIR spectra of (a) PCL/Nyst and (b) PLA/PCL/Nyst composites. [Color figure can be viewed at wileyonlinelibrary.com]
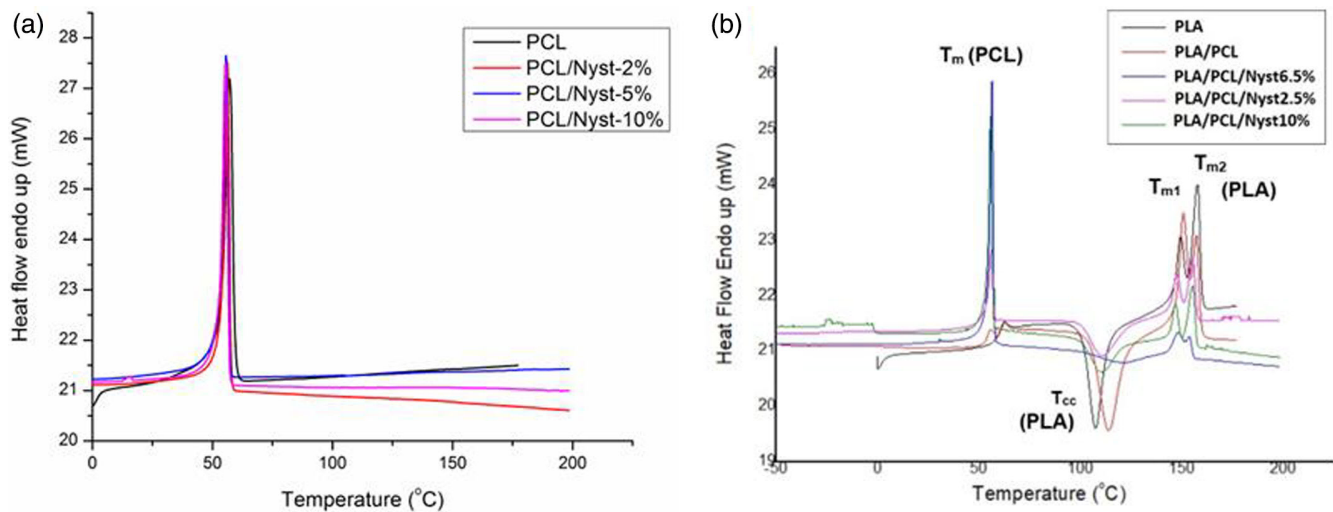
FIGURE 2 Second heating curves of (a) PCL/Nyst and (b) PLA/PCL/Nyst composites. [Color figure can be viewed at wileyonlinelibrary.com]

PCL/Nyst within the PLA matrix depends on the nature of the polymer, their polar surface functionalities, duration of mixing, and the compatibility between PCL/Nyst and PLA matrix. A calculated amount of PCL/Nyst composites is blended with PLA to form 3 different types of PLA/PCL/Nyst composites, which were encoded as PLA/PCL/Nyst2.5%, PLA/PCL/Nyst6.5%, and PLA/PCL/Nyst10%, each containing 2.5%, 6.5%, and 10% nystatin,
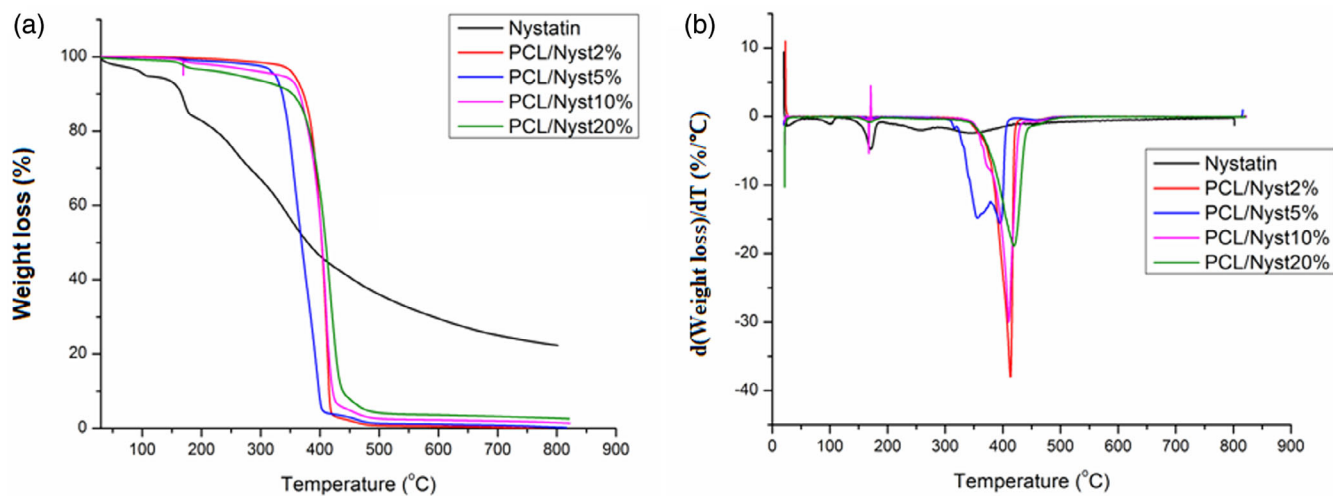
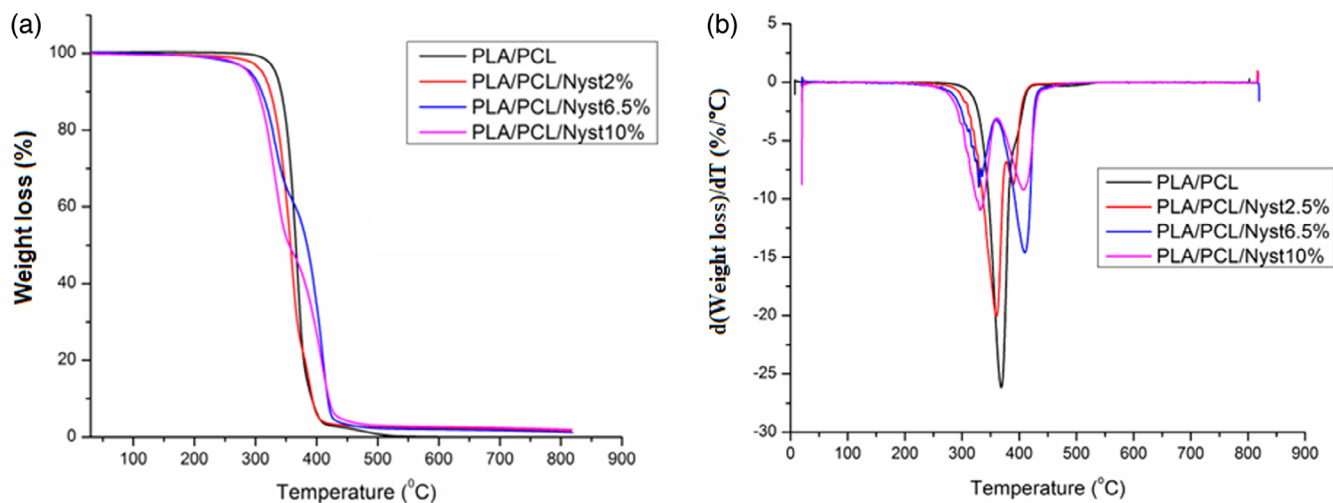**FIGURE 3** (a) TGA thermograms and (b) DTG curves of PCL/Nyst composites. [Color figure can be viewed at wileyonlinelibrary.com]

FIGURE 4 (a) TGA thermograms and (b) DTG curves of PLA/PCL/Nyst composites. [Color figure can be viewed at wileyonlinelibrary.com]

TABLE 4 Thermal degradation parameters and melting temperatures of PLA/PCL/Nyst composites.

Parameter		PLA/PCL	PLA/PCL/Nyst2.5%	PLA/PCL/Nyst6.5%	PLA/PCL/Nyst10%
Onset temperature (°C)		302	279	268	247
Peak temperature for 1st stage degradation (°C)		368	359	331	332
Peak temperature for 2nd stage degradation (°C)		–	388	409	407
T_{cc} (PLA) (°C)		121.71	111	120.94	110.53
T_c (PLA) (°C)		34.82	30.52	35.71	26.14
Char residue (%)		0	1.7	1.16	2.0
Melting temperature (T_m)	T_{m1}	151	147	148	147
	T_{m2}	157	155	153	155
ΔHm (PLA) (J/g)		16.44	14.11	8.89	12.75
X_c (PLA) (% crystallinity)		22	20	14	27.21

respectively, using a master batch approach. Table 3 shows the required amount of PLA and PCL/Nyst to prepare PLA/PCL/Nyst composites. For example, PLA/PCL/Nyst2.5% was prepared by melt-mixing PCL/Nyst10% composite with PLA. As given in Table 1, PCL/Nyst10% contain 90% PCL and 10% nystatin. So, for a 40 g batch we used 10 g PCL/Nyst10% (10 g PCL/Nyst10% = 9 g PCL + 1 g nystatin) composite and 30 g of PLA for melt-blending which gives the final composite PLA/PCL/Nyst2.5%, containing 2.5% nystatin.

3.2 | Characterization of PLA/PCL/Nyst composites

FTIR studies were performed to understand the interaction of nystatin with PLA and PCL (Figure 1). Nystatin has characteristic absorption bands were noted at 3377.20, 2935.12, 1705.36, 1442.56, 1322.0, and 1063.84 cm^{-1}.[45] From the FTIR spectra of PCL/Nyst, it was observed that the absorption band at 3331–3348, absorption peaks at 2858–2941, 1725, 1361–1424, 1158–1228 cm^{-1} are attributed to C—H, C=O carbonyl, C—O of saturated ester stretching and bending of C—O—H peaks, respectively[46] (Figure 1a). Similarly, the FTIR spectra of PLA/PCL/Nyst composites show absorptions bands at 3334–3423, 2859–2933, 1715, 1180, and 1417–1448 cm^{-1}, attributed to O—H and N—H stretching, C—H, C=O carbonyl, C—O of saturated ester stretching, C—O—H bending, respectively (Figure 1b). These interfacial interactions play a fundamental role in the uniform distribution of nystatin over the polymeric matrix, as nystatin possesses an intrinsic affinity to interact with PLA and PCL either non-covalently or covalently by its available amine residue.[45,47]

The DSC analysis was performed to understand the incorporation of nystatin on the composites thermal properties (melting point, T_m). From the DSC analysis, we noted that PCL/Nyst composites with various amounts of nystatin did not show significant variation in the melting of point of the composites (T_m: 55–56°C) (Figure 2a). On the other hand, the DSC analysis of PLA/PCL/Nyst composites shows two melting peaks around 56°C and between 147 and 157°C, corresponding to PCL and PLA, respectively (Figure 2b). The variation in the T_m of PLA may be due to the existence of two diverse type of PLA crystals with different perfection within the blend system.[47] Furthermore, with an increase in PCL/Nyst content in the blend, the T_m of PLA decreases compared to Tm of PLA in the PLA/PCL/Nyst blend. This may be attributed to the amorphous soluble fraction of nystatin that is miscible in the PLA phase; or the soluble fraction of nystatin that is miscible in PCL. The glass transition temperature (T_g) of the neat PLA was found by 60.2°C, however, the peak is not identifiable in the blend system due to overlap with the PCL melting point, as shown in Figure 2b.[48]
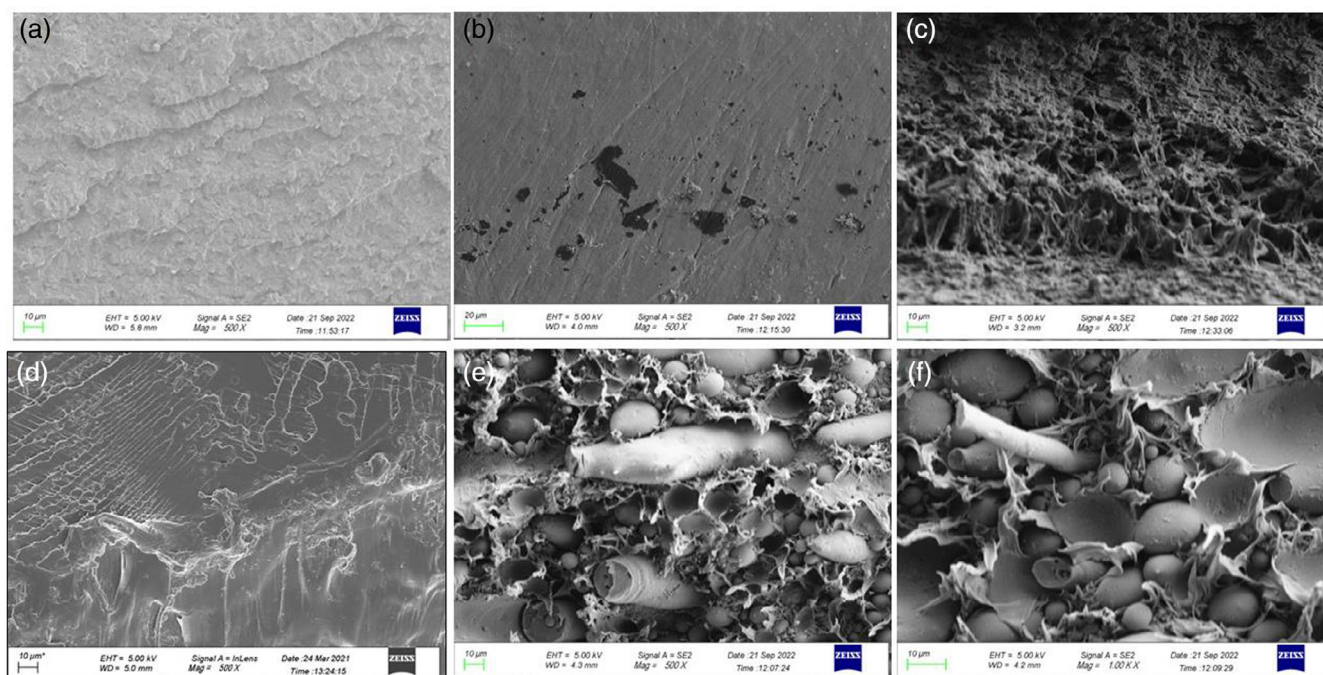

FIGURE 5 Cross-section scanning electron micrographs for (a) PCL; PCL/Nyst5% (c) PCL/Nyst20% (d) PLA; PLA/PCL/Nyst2.5% at magnification (e)500× and (f)1000×. [Color figure can be viewed at wileyonlinelibrary.com]

Thermal degradation nystatin, PCL/Nyst and PLA/PL/Nyst composites were performed and TGA thermograms and first derivative curves (dTG) are presented in Figures 3 and 4. At about 90°C, a 3–5 wt% loss was observed for nystatin due to the loss of volatiles and moisture. Nystatin starts to degrade at a temperature above 170°C and degrades rapidly, mainly due to structural decomposition. At the end of the analysis at 800°C, around 30% of non-combusted material was observed. This may be due to the crosslinking and carbonization of aromatics present in the nystatin.[49]

Similarly, 3–5 wt% of initial loss was observed for PCL/Nyst composites, as seen in nystatin (Figure 3a), and the degradation temperature was varied for the
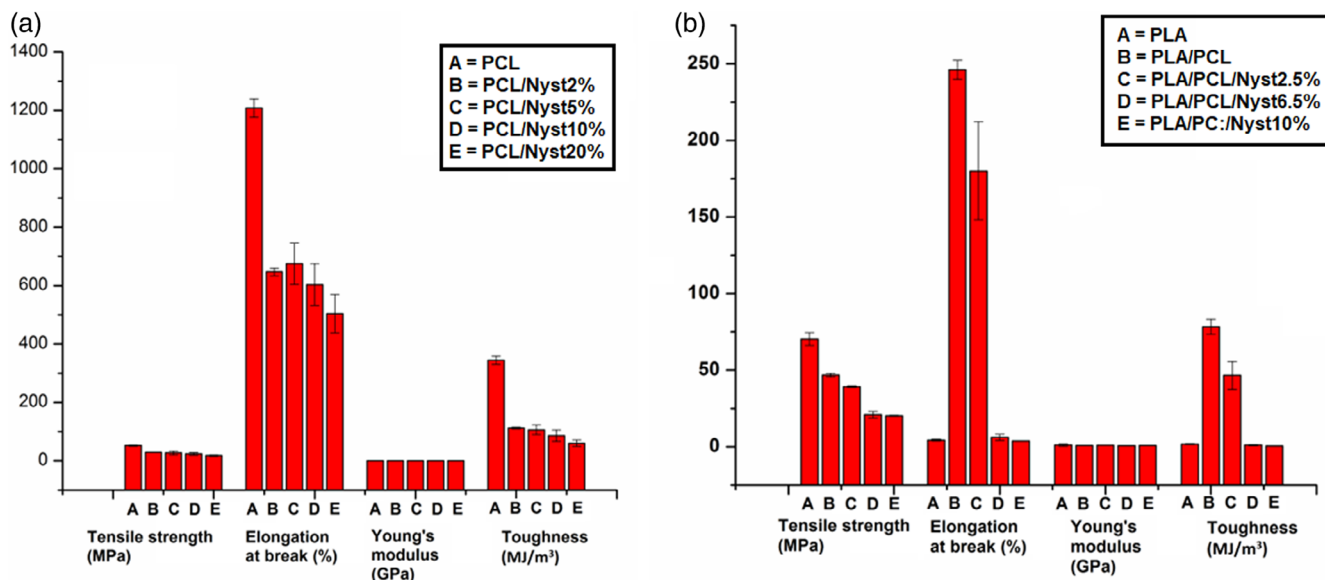

FIGURE 6 Comparison of mechanical properties of (a) PCL/Nyst (b) PLA/PCL/Nyst composites. [Color figure can be viewed at wileyonlinelibrary.com]
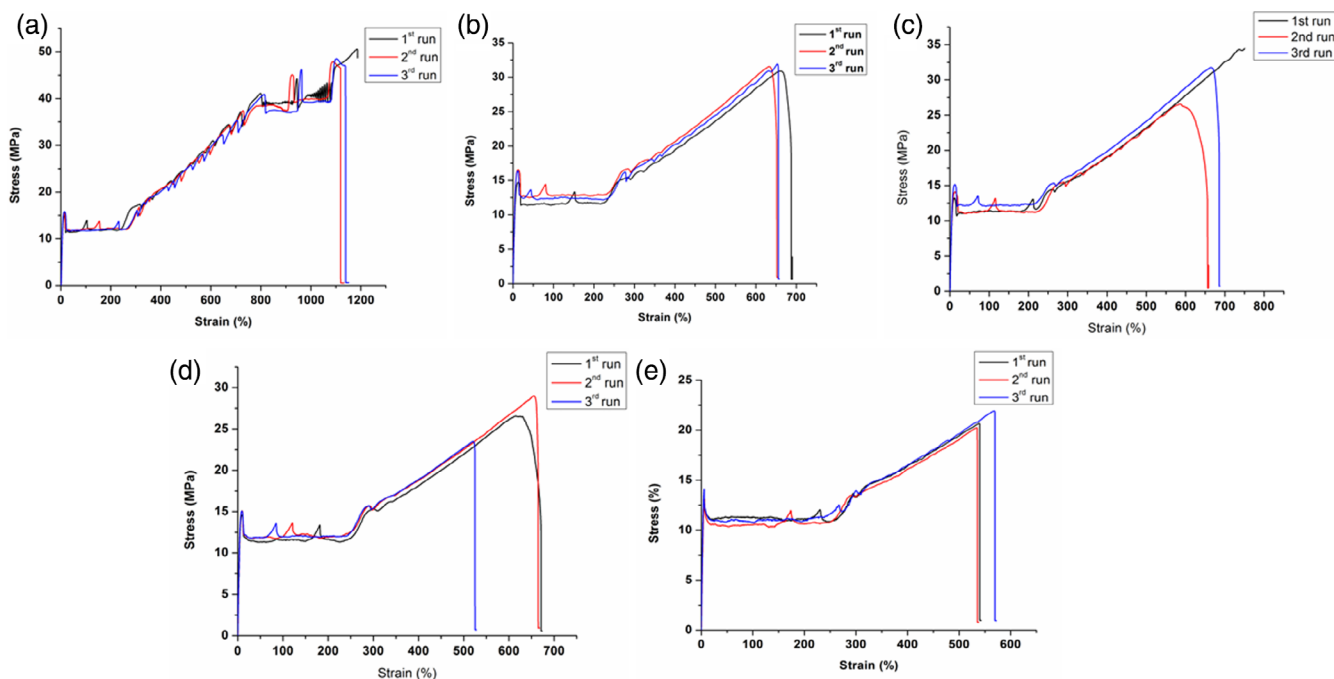

FIGURE 7 Stress–strain profiles of (a) PCL, (b) PCL/Nyst2%, (c) PCL/Nyst5%, (d) PCL/Nyst10%, (e) PCL/Nyst20%. [Color figure can be viewed at wileyonlinelibrary.com]
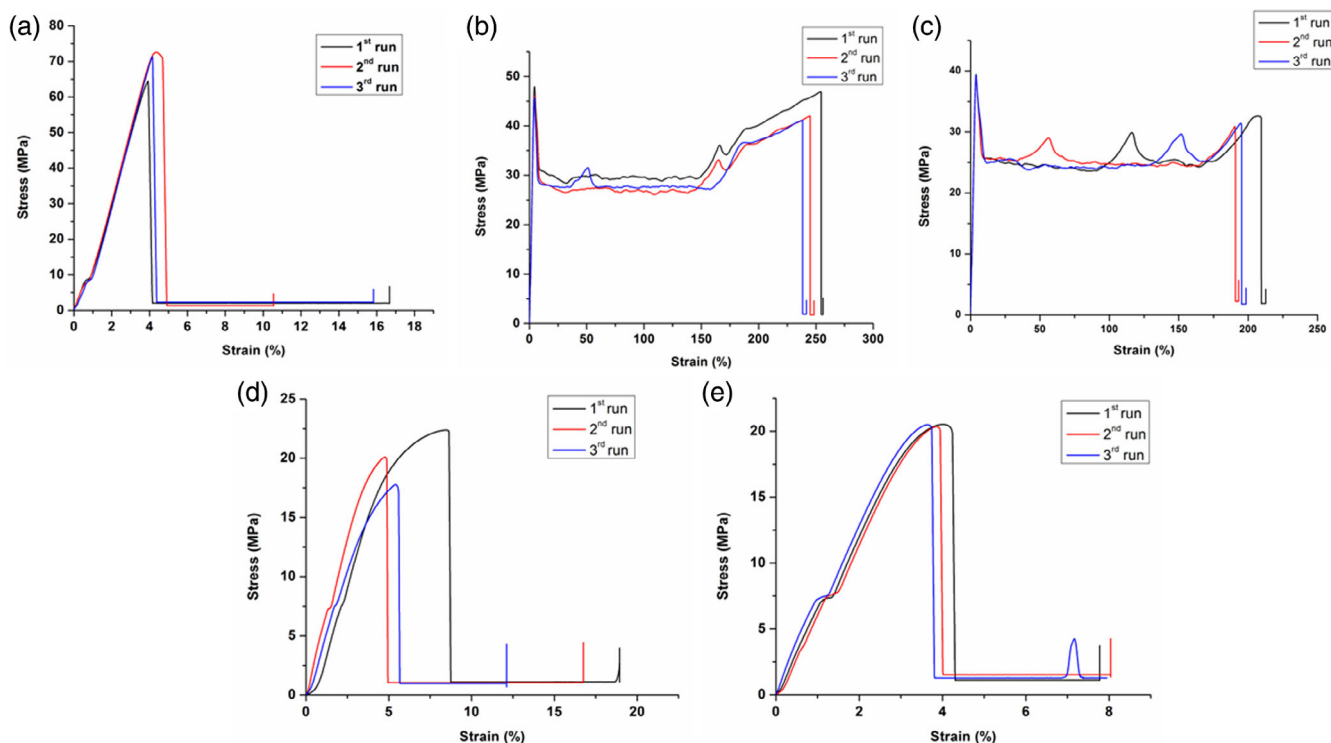
FIGURE 8 Stress–strain profiles of (a) PLA, (b) PLA/PCL, (c) PLA/PCL/Nyst2.5%, (d) PLA/PCL/Nyst6.5%, (e) PLA/PCL/Nyst10%. [Color figure can be viewed at wileyonlinelibrary.com]

TABLE 5 Mechanical properties of PLA/PCL composites with nystatin (average of 3 runs).

Samples	Tensile strength, MPa		Elongation at break, %		Young's modulus, (GPa)		Toughness (MJ/m^3)[a]	
	Average	G[b]	Average	G	Average	G	Average	G
PCL	49.15 ± 1.46	E_1	1148.46 ± 36.02	D_2	0.23 ± 0.015	A_3	316.89 ± 19.63	F_4
PCL/Nyst2%	31.26 ± 0.64	C_1	649.7 ± 14.23	C_2	0.30 ± 0.01	A_3	124.3 ± 2.7	E_4
PCL/Nyst5%	31 ± 4.02	C_1	690.83 ± 51.83	C_2	0.27 ± 0.01	A_3	130.11 ± 17.55	E_4
PCL/Nyst10%	26.20 ± 3.06	B_1	601 ± 71.61	C_2	0.34 ± 0.023	A_3	104.14 ± 20	D_4
PLA/Nyst20%	21 ± 0.85	A_1	547.78 ± 17	C_2	0.44 ± 0.05	A_3	76.08 ± 4.83	C_4
PLA	69.61 ± 4.42	F_1	4.26 ± 0.40	A_2	1.32 ± 0.09	D_3	1.71 ± 0.20	A_4
PLA/PCL	46.6 ± 1.22	E_1	246.18 ± 7.9	B_2	0.86 ± 0.02	B_3	78.26 ± 7.06	C_4
PLA/PCL/Nyst2.5	39.30 ± 0.05	D_1	198.56 ± 9.4	B_2	1.01 ± 0.08	C_3	51.03 ± 2.70	B_4
PLA/PCL/Nyst6.5%	20.05 ± 2.3	A_1	6.39 ± 2	A_2	0.53 ± 0.13	A_3	0.90 ± 0.38	A_4
PLA/PCL/Nyst10%	20.42 ± 0.03	A_1	3.98 ± 0.24	A_2	0.78 ± 0.03	B_3	0.52 ± 0.02	A_4

[a]Calculated by integrating the area under stress–strain curves.
[b]The average with different letters in a particular column belongs to different populations and have a statistically significant difference between them (ANOVA test and post-hoc Fisher's LSD test, $p \leq 0.05$ was considered statistically significant). Subscript denotes column number.

PCL/Nyst composites (Figure 3b). With increasing nystatin concentration, the thermal degradation temperature of the composites was increased mainly due to the increased concentration of nystatin in the composites. As a result, the onset degradation temperature of PLA/PCL/Nyst composites was lower than PLA/PCL composites, as shown in Table 4 and Figure 4a. The onset degradation temperature of

PLA/PCL composites was 306°C and for the PLA/PCL/Nyst composites, it varied from 247 to 279°C depending on the amount of nystatin present in the composites. This variation may be due to the loss of volatile, moisture and weaker interaction between the polymers and nystatin. Both PCL/Nyst and PLA/PCL/Nyst composites showed two-step thermal degradation profiles (Figures 3b and 4b).

3.3 | SEM analysis

The prepared melt-processed nystatin-based composites were smooth, transparent, and devoid of cracks. In addition, cross-section SEM morphology of the composites was carried out to understand the effect of nystatin in PCL; and PCl/Nyst in PLA matrix and to determine the relation between the cross-section morphology and mechanical properties of the composites (Figure 5).

The SEM image of the fractured surface of neat PCL was dense and compact with no apparent pores and visible plastic deformation, indicating that the film was fractured under a brittle mode[48] (Figure 5a). The uniform surface is devoid of any pores, which explains its very high elongation at break. The cross-section morphologies of the PCL film exhibited apparent change with an increase in the incorporation of nystatin. 5% addition of nystatin to PCL shows a homogeneous and smooth surface, consistent with brittle behavior, and did not modify the cross section of PCL (Figure 5b). However, with the increased addition of nystatin from 5% to 20%, there is a slight increase in roughness and irregularities in the cross-sections (Figure 5c).

The SEM images of the fractured surface of neat PLA were smooth, indicating a brittle rupture (Figure 5d). In contrast, with the incorporation of PCL/Nyst in PLA, there is an increase in roughness and irregularities in the cross-section of PLA/PCL/Nyst2.5% (Figure 5e,f). In addition, we can also observe spherical droplets of PCL distributed within the PLA matrix. This is attributed to the low T_m (57.3°C) of PCL which results in complete melting of PCL at the mixing stage and shearing to tiny droplets.[39,50] Thus, the most marked differences in the film structures were observed for the samples containing nystatin, where diverse networks was observed. Moreover, there is no sign of agglomeration of nystatin within the polymer matrix, confirming its uniform dispersion.

3.4 | Mechanical strength of the materials

Generally, packaging applications demand good strength, toughness, and flexibility of the material. Unfortunately, biodegradable, bio-based polymeric material alone cannot offer adequate strength and bioactivity as a suitable packaging material. Packaging films with low tensile strength tend to break during use under a certain load. The mechanical properties of the composites are determined and tabulated in Table 4 and shown in Figure 6. From the cross-section SEM images of fractured surface of PCL/Nystatin composites (Figure 5a–c), we observed that nystatin was uniformly distributed in the polymeric

matrix with no sign of agglomeration. As PLA, PCL and nystatin contain many polar functional groups, they can interact effectively via physico-chemical interactions.[51] However, increasing amounts of nystatin leads to decreased tensile strength, elongation at break, and toughness of neat PCL, which shows that nystatin does not act as a nucleating agent. Upon blending 10 g of PCL/Nyst10% with PLA to obtain PLA/PCL/Nyst2.5%, the elongation is higher than that of neat PLA. However, on further increase in nystatin content (6.5% to 10%) in PLA/PCL/Nyst composites, the tensile strength, elongation at break and toughness decreases. This is attributed
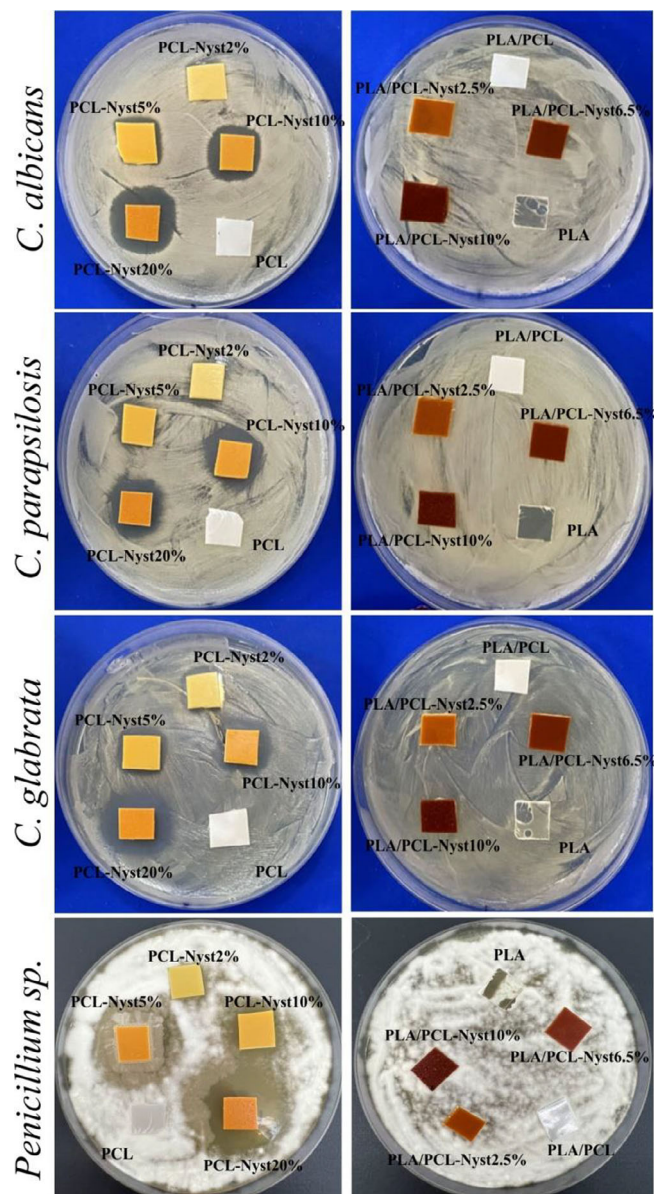

FIGURE 9 Antifungal activity assay, direct application of plastic materials on growth medium with three different *Candida* species and *Penicillium* sp. [Color figure can be viewed at wileyonlinelibrary.com]

to the fact that 2.5% nystatin might be the optimum amount for improvement in elongation at break of PLA with the presence of an optimum number of polar functional groups to help provide strong interfacial interactions of nystatin within the polymeric matrix.[52]

The stress–strain profiles of PCL/Nyst and PLA/PCL/ Nyst composites are shown in Figures 7 and 8, respectively. The statistical analysis of the mechanical properties was also performed, using ANOVA test and post-hoc Fisher's LSD test where $p \leq 0.05$ was considered statistically significant. As shown in Table 5, composites with significantly different mechanical properties are classified in a particular column using similar letters. In other words, the average values of the composites for a specific mechanical property denoted with the same letter, such as A_1 belong to the same population with no difference among them. However, there is a statistically significant difference between average values labeled "A_1" and average values labeled "B_1" (where the subscript denotes column number).

Figures 7 and 8 show the triplicate measurements of stress–strain profile of various PLA, PCL, and Nystain composites.

3.5 | Antifungal activity of nystatin containing materials

For the assessment of antifungal activity in direct assay, plastic materials were placed on the growth medium where different *Candida* strains and foodborne *Penicillium*

sp. were spread, and the zone of inhibition was observed. While a mixture of PLA/PCL/Nyst composites did not have any antifungal activity on all tested strains in this direct assay, PCL/Nyst20% had a major impact on to the growth of all tested *Candida* species. PCL/Nyst20%, the material with the highest percentage of nystatin, was the most potent material in this study, inhibiting the growth of all tested *Candida* strains and *Penicillium* sp. with the zones diameter between 4 and 21 mm (Figure 9).

The PCL with a lower nystatin percentage had notable activity but smaller inhibition zones compared to PCL/Nyst20%. Foodborne fungi *Penicillium* sp. was the most sensitive to PCL-Nys materials with the widest zone diameters for all nystatin percentages (Figure 9, bottom left). It has been previously shown that nystatin causes foodborne Penicillium sp. membrane disruption.[48]

With the aim of more detailed antifungal activity study and toxicity assessment, materials were incubated in a growth medium, and these extracts were further tested to establish inhibitory potential. With 50% of material extracts in total well volumes, all the PCL/Nyst materials inhibited the growth of all tested *Candida* strains for more than 50%, with the highest impact on *C. albicans* strain (Figure 10). Materials with the highest concentration of nystatin were also the most active one in this assay. Noteworthy is the antifungal effect of the material extract containing no antifungals, especially of the PCL that inhibited fungal growth by 50%–70% in comparison to the control (Figure 10). Importantly, no toxicity of these extracts was detected in vivo toward
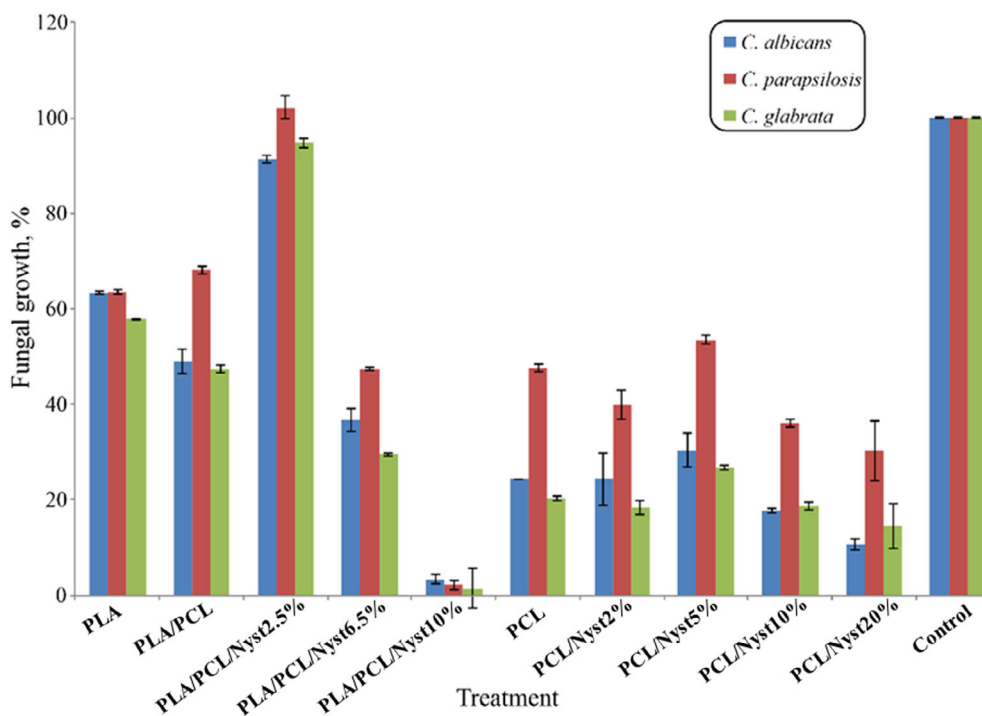
FIGURE 10 Materials extract impact on *C. albicans*, *C. parapsilosis*, and *C. glabrata* growth. Strains were grown in medium containing 50% (v/v) of material extracts. [Color figure can be viewed at wileyonlinelibrary.com]

FIGURE 11 Release of nystatin in PBS from nystatin-based composites at 37–39°C, over a period of 4 days. Values are the average of two separate experiments ± standard. deviations (*SD*). [Color figure can be viewed at wileyonlinelibrary.com]
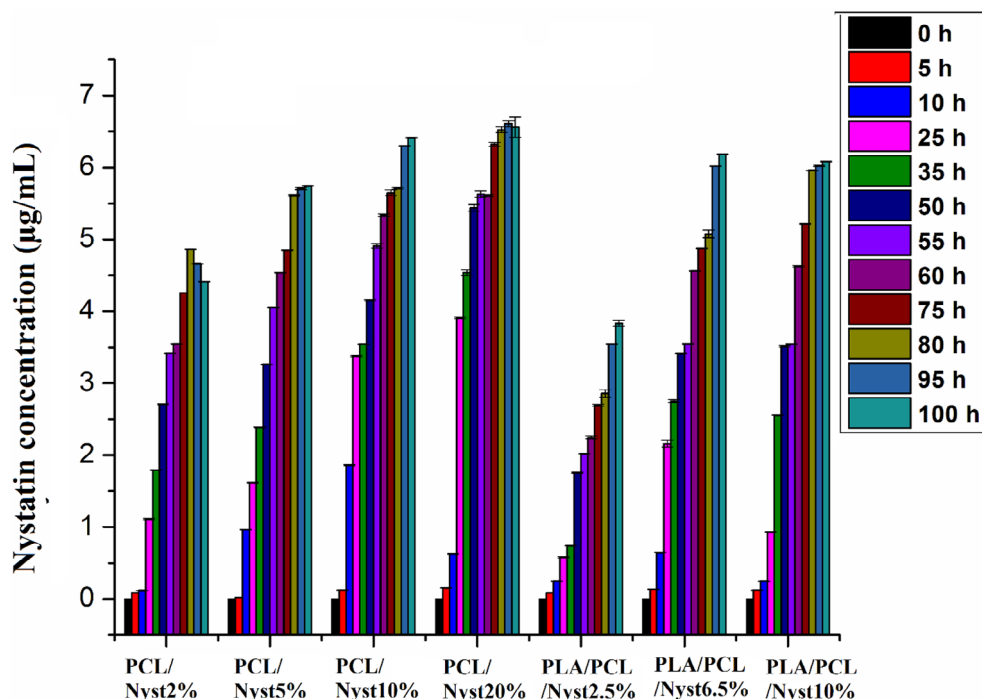
C. elegans and they did not interact with worms′ activity even at the highest tested concentration of 100%, v/v (data not shown). *C. elegans* is very often used as a model for antifungal drug discovery.[52]

The antifungal activity of PCL materials coated with nystatin has been also reported previously where authors made membrane with PCL, 4,4′-diphenyl methane diisocyanate and hydroxypropyl cellulose supplemented with nystatin.[53] PCL was also chosen for the nanocapsules preparation to make nystatin nanocapsular hydrogel for the treatment of topical candidiasis in comparison to commercially available nystatin hydrogen. Nys-NC6 composed of 0.25% w/w PCL, 5% w/w squalene, and 1% w/w Sp60 showed the most favorable attributes.[54] Also, medium chain length polyhydroxyalkanoates (mcl-PHA) were used to formulate both polyenes (Nys and AmB) in the form of films and showed excellent growth inhibitory activity against two *C. albicans* strains, *C. parapsilosis* and on several filamentous fungi including *Microsporum gypseum*.[26]

3.6 | Release kinetics of nystatin

To determine the potential application of the composite films as a packaging material against fungal infection, the release of nystatin was carried out in PBS solution at pH 5.5 and pH 7 at 37–39°C over a period of 4 days. UV/Vis spectroscopy was used to determine the release of nystatin (at $\lambda_{max} = 290$ nm) from the films over a period of 4 days. The release profiles of nystatin from the PLA/PCL/Nyst and PCL/Nyst composites are shown in Figure 11. The composites exposed to pH 7 environments

showed the release of nystatin over the course of 4–5 days. Again, the release rate of nystatin from the PLA/PCL/Nyst composite was slower than that from PCL/Nyst, which indicates that the composites have the prospective to be utilized for the controlled release of antimicrobial agents. This result may be attributed to the interaction between the oxygeneous groups of nystatin with PLA/PCL matrix. These data also support our findings that in the direct assay, no zones of inhibition were detect in the case of PLA/PCL/Nyst materials (Figure 9), while in the case when materials extracts were applied to the fungal cultures, growth inhibition occurred (Figure 10).

4 | CONCLUSION

The present work demonstrated a conventional high-processivity melt-processing of bio-based polymers with natural polyene (nystatin) to produce antifungal films, for the first time. The composites showed enhanced antifungal activity for all PCL/Nystatin composites on three *Candida* strains and foodborne *Penicillium* sp. The blend composites, PLA/PCL/Nyst showed complete growth inhibition at 50% volume of material extract in the indirect assay and proved to be potential in packaging applications for liquid substances. All PCL/Nyst composites showed better mechanical properties compared to pristine PLA. However, increasing the blend's polyene content decreases the blend composite's mechanical strength. Thus, the present work demonstrates the production of biodegradable polymer composites with naturally derived polyene using a melt processing technique that can be adoptable on an industrial

scale. This study will pave the way for developing sustainable, antibacterial, and biodegradable plastic food packaging films that can enhance food product's shelf life and reduce plastic waste.

AUTHOR CONTRIBUTIONS

Ramesh Babu Padamati: Conceptualization (lead); funding acquisition (lead); supervision (lead); writing – review and editing (equal). **Rituparna Duarah:** Data curation (equal); formal analysis (lead); investigation (lead); writing – original draft (lead). **Ivana Aleksic:** Formal analysis (lead); methodology (lead); validation (equal); writing – original draft (equal). **Dusan Milivojevic:** Formal analysis (lead); investigation (lead); methodology (lead); validation (lead); writing – original draft (supporting). **Saranya Rameshkumar:** Validation (supporting); writing – review and editing (supporting). **Jasmina Nikodinovic-Runic:** Conceptualization (lead); funding acquisition (lead); methodology (lead); project administration (lead); supervision (lead); writing – original draft (supporting); writing – review and editing (supporting).

ACKNOWLEDGMENTS

CONFLICT OF INTEREST STATEMENT

The Authors confirm there is no conflict of interest associated with manuscript.

DATA AVAILABILITY STATEMENT

The data that support the findings of this study are available from the corresponding author upon reasonable request.

ORCID

Rituparna Duarah https://orcid.org/0000-0002-7989-5745

Ivana Aleksic https://orcid.org/0000-0001-5635-0024

Dusan Milivojevic https://orcid.org/0000-0003-1264-1780

Ramesh Babu Padamati https://orcid.org/0000-0003-0102-0049

REFERENCES

[1] W. Ntow-Boahene, D. Cook, L. Good, *Front. Bioeng. Biotechnol.* **2021**, *9*, 780328.

[2] E. Sánchez-López, D. Gomes, G. Esteruelas, L. Bonilla, A. L. Lopez-Machado, R. Galindo, A. Cano, M. Espina, M. Ettcheto, A. Camins, *Nanomaterials* **2020**, *10*, 292.

[3] K. L. Yam, S. L. Dong, *Emerging Food Packaging Technologies: Principles and Practice*, Elsevier, Cambridge, UK **2012**.

[4] https://www.unep.org/resources/report/unep-food-waste-index-report-2021.

[5] R. Chawla, S. Sivakumar, H. Kaur, *Carbohydr.Polymer Technol. Appl.* **2021**, *2*, 100024.

[6] M. S. Firouz, K. Mohi-Alden, M. Omid, *Food Res. Int.* **2021**, *141*, 110113.

[7] F. Wu, M. Misra, *Prog. Polym. Sci.* **2021**, *117*, 101395.

[8] M. Y. Khalid, Z. U. Arif, *Food Packag. Shelf Life* **2022**, *33*, 100892.

[9] S. Maisanaba, M. Llana-Ruiz-Cabello, D. Gutiérrez-Praena, S. Pichardo, M. Puerto, A. I. Prieto, A. Jos, A. M. Cameán, *Food Rev. Int.* **2017**, *33*, 447.

[10] A. Samir, F. H. Ashour, A. A. A. Hakim, M. Bassyouni, *Npj Mater. Degrad.* **2022**, *6*, 68.

[11] T. Gérard, T. Budtova, *Proceedings of the International Conference on Biodegradable and Biobased Polymers-BIOPOL*, Strasbourg, France **2011**.

[12] I. Armentano, E. Fortunati, N. Burgos, F. Dominici, F. Luzi, S. Fiori, A. Jiménez, K. Yoon, J. Ahn, S. Kang, J. M. Kenny, *Express Polym. Lett.* **2015**, *9*, 583.

[13] J. Li, X. Luo, X. Lin, Y. Zhou, *Starch/Staerke* **2013**, *65*, 831.

[14] M. Rajendran, M. Manjusri, K. M. Ama, *J. Appl. Polym. Sci.* **2018**, *135*, 1.

[15] Y. Han, J. Shi, L. Mao, Z. Wang, L. Zhang, *Ind. Eng. Chem. Res.* **2020**, *59*, 21779.

[16] T. T. Thiyagu, J. V. S. Kumar, P. Gurusamy, V. Sathiyamoorthy, T. Maridurai, A. V. R. Prakash, *Biomass Convers. Biorefin.* **2021**, *13*, 11841.

[17] I. R. Sousa Vieira, A. P. A. de de Carvalho, C. A. Conte-Junior, *Compr. Rev. Food Sci. Food Saf.* **2022**, *21*, 3673.

[18] L. Zhou, H. He, M. C. Li, S. Huang, C. Mei, Q. Wu, *Ind. Crops. Prod.* **2018**, *112*, 449.

[19] M. Jordá-Reolid, A. Ibáñez-García, L. Catani, A. Martínez-García, *Polymers* **2022**, *14*, 5223.

[20] J. J. Koh, X. Zhang, *Int. J. Biol. Macromol.* **2018**, *109*, 99.

[21] R. Muthuraj, M. Misra, A. K. Mohanty, *J. Appl. Polym. Sci.* **2018**, *135*, 45726.

[22] J. M. Ferri, D. Garcia-Garcia, L. Sánchez-Nacher, O. Fenollar, R. Balart, *Carbohydr. Polym.* **2016**, *147*, 60.

[23] C. L. Reichert, E. Bugnicourt, M. B. Coltelli, P. Cinelli, A. Lazzeri, I. Canesi, F. Braca, B. M. Martínez, R. Alonso, L. Agostinis, S. Verstichel, *Polymers* **2020**, *12*, 1558.

[24] S. C. Chen, T. C. Sorrell, *Med. J. Aust.* **2007**, *187*, 404.

[25] L. J. Bastarrachea, D. E. Wong, M. J. Roman, Z. Lin, J. M. Goddard, *Coatings* **2015**, *5*, 771.

[26] M. Pekmezovic, M. K. Krusic, I. Malagurski, J. Milovanovic, K. Stępień, M. Guzik, R. Charifou, R. Babu, K. O'Connor, J. Nikodinovic-Runic, *Antibiotics* **2021**, *10*, 737.

[27] S. H. Kamarudin, M. Rayung, F. Abu, S. Ahmad, F. Fadil, A. A. Karim, M. N. Norizan, N. Sarifuddin, M. S. Z. M. Desa, M. S. M. Basri, H. Samsudin, L. C. Abdullah, *Polymers* **2022**, *14*, 174.

[28] V. G. Ibarra, A. R. B. R. Sendón, V. de Quirós, in *Antimicrobial Food Packaging* (Ed: J. Barros-Velázquez), Academic Press, San diego, CA **2016** Ch. 29.

[29] A. M. Bargan, G. Ciobanu, C. Luca, M. Diaconu, I. G. Sandu, *Materiale Plastice* **2014**, *51*, 167.

[30] J. Wangprasertkul, R. Siriwattanapong, N. Harnkarnsujart, *Food Control* **2021**, *123*, 107763.

[31] T. Haro-Reyes, L. Díaz-Peralta, A. Galván-Hernández, A. Rodríguez-López, L. Rodríguez-Fragoso, I. Ortega-Blake, *Membranes* **2022**, *12*, 681.

[32] A. Beltrán Sanahuja, A. Valdés García, *Polymer* **2021**, *13*, 1053.

[33] S. Manso, R. Becerril, C. Nerín, R. Gómez-Lus, *Food Control* **2015**, *47*, 20.

[34] L. Gutierrez, A. Escudero, R. Batle, C. Nerin, *J. Agric. Food Chem.* **2009**, *57*, 8564.

[35] P. López, C. Sánchez, R. Batlle, C. Nerín, *J. Agric. Food Chem.* **2007**, *55*, 8814.

[36] M. Rujnić-Sokele, A. Pilipović, *Waste Manage. Res.* **2017**, *35*, 132.

[37] A. K. Matta, R. U. Rao, K. N. S. Suman, V. Rambabu, *Proc. Mater. Sci.* **2014**, *6*, 1266.

[38] S. Parameswaran, B. B. Dorian, R. Senthamaraikannan, R. B. Padamati, *Molecules* **2020**, *25*, 5766.

[39] M. Przybysz-Romatowska, J. Haponiuk, K. Formela, *Polymers* **2020**, *12*, 228.

[40] N. G. Heatley, *Biochem. J.* **1944**, *38*, 61.

[41] M. M. Weerasekera, G. K. Wijesinghe, T. A. Jayarathna, C. P. Gunasekara, N. Fernando, N. Kottegoda, L. P. Samaranayake, *Mem. Inst. Oswaldo Cruz.* **2016**, *111*, 697.

[42] M. C. Arendrup, M. Cuenca-Estrella, C. Lass-Flörl, W. Hope, *Clin. Microbiol. Infect.* **2012**, *18*, 246.

[43] T. Stiernagle, *Maintenance of C. elegans*, *WormBook*, ed. The C. elegans Research Community, WormBook, Minneapolis, USA **2006**, p. 1.

[44] M. Djapovic, D. Milivojevic, T. Ilic-Tomic, M. Lješević, E. Nikolaivits, E. Topakas, V. Maslak, J. Nikodinovic-Runic, *Chemosphere* **2021**, *275*, 130005.

[45] A. I. El-Batal, H. G. Nada, R. R. El-Behery, M. Gobara, G. S. El-Sayyad, *RSC Adv.* **2020**, *10*, 9274.

[46] T. Kemala, E. Budianto, B. Soegiyono, *Arab. J. Chem.* **2012**, *5*, 103.

[47] M. Dadras Chomachayi, A. Jalali-Arani, F. R. Beltrán, M. U. de la Orden, J. M. Urreaga, *J Polym. Environ.* **2020**, *28*, 1252.

[48] S. Wachirahuttapong, C. Thongpin, N. Sombatsompop, *Energy Procedia* **2016**, *89*, 198.

[49] S. H. Hussein-Al-Ali, M. E. I. Zowalaty, A. U. Kura, B. Geilich, S. Fakurazi, T. J. Webster, M. Z. Hussein, *BioMed Res. Int.* **2014**, *2014*, 651831.

[50] T. Patrício, P. Bártolo, *Procedia Eng.* **2013**, *59*, 292.

[51] M. Mandru, C. Ciobanu, M. E. Ignat, M. Popa, L. Verestituc, S. Vlad, *Dig. J. Nanomater. Biostruct.* **2011**, *6*, 127.

[52] M. R. Van Leeuwen, E. A. Golovina, J. Dijksterhuis, *J. Appl. Microbiol.* **2009**, *106*, 1908.

[53] M. Mandru, *Cellulose Chem. Technol.* **2013**, *47*, 5.

[54] M. M. AbouSamra, M. Basha, G. E. A. Awad, S. S. Mansy, *J Drug Deliv. Sci. Technol.* **2019**, *49*, 365.